THE JOURNAL OF PHYSICAL CHEMISTRY B

Article

Cite This: J. Phys. Chem. B 2018, 122, 1334−1344

pubs.acs.org/JPCB

Extraction of Gd^{3+} and UO_2^{2+} Ions Using Polystyrene Grafted Dibenzo Crown Ether (DB18C6) with Octanol and Nitrobenzene: A Molecular Dynamics Study

Praveenkumar Sappidi,[†] Sadanandam Namsani,[†] Sk. Musharaf Ali,[*,‡] and Jayant Kumar Singh[*,†]

[†]Computational Nano Science Laboratory, Department of Chemical Engineering, Indian Institute of Technology (IIT) Kanpur, Kanpur 208016, India

[‡]Chemical Engineering Division, Bhabha Atomic Research Center, Mumbai 400085, India

Supporting Information

ABSTRACT: Atomistic molecular dynamics (MD) simulations are performed in order to derive thermodynamic properties important to understand the extraction of gadolinium (Gd^{3+}) and uranium dioxide (UO_2) with dibenzo crown ether (DBCE) in nitrobenzene (NB) and octanol (OCT) solvents. The effect of polystyrene graft length, on DBCE, on the binding behavior of Gd^{3+} and UO_2^{2+} is investigated for the first time. Our simulation results demonstrate that the binding of Gd^{3+} and UO_2^{2+} onto the oxygens of crown ethers is favorable for polystyrene grafted crown ether in the organic solvents OCT and NB. The metal ion binding free energy ($\Delta G_{Binding}$) in different solvent environments is calculated using the thermodynamic integration (TI) method. $\Delta G_{Binding}$ becomes more favorable in both solvents, NB and OCT, with an increase in the polystyrene monomer length. The metal ion transferability from an aqueous phase to an organic phase is estimated by calculating transfer free-energy calculations ($\Delta G_{Transfer}$). $\Delta G_{Transfer}$ is significantly favorable for both Gd^{3+} and UO_2^{2+} for the transfer from the aqueous phase to the organic phase (i.e., NB and OCT) via ion-complexation to DBCE with an increase in polystyrene length. The partition coefficient (log P) values for Gd^{3+} and UO_2^{2+} show a 5-fold increase in separation capacity with polystyrene grafted DBCE. We corroborate the observed behavior by further analyzing the structural and dynamical properties of the ions in different phases.

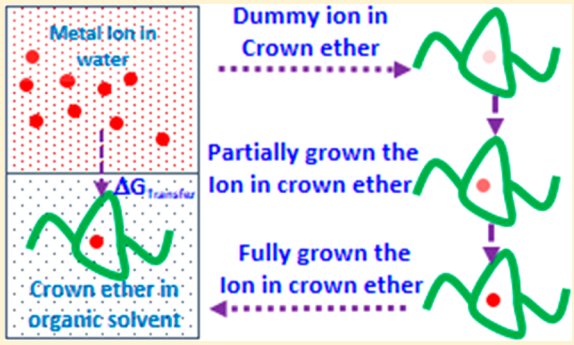

1. INTRODUCTION

Separation of heavy metal ions from contaminated wastewater is a very important and challenging problem in the world. The high level radioactive waste contains lanthanide gadolinium (Gd^{3+}) and uranyl (UO_2^{2+}) ions, which are toxic in nature, and thus, extraction of these ions from the nuclear waste is warranted. One commonly used separation method is liquid−liquid extraction, where a suitable extractant is used to bind the metal ion in the form of complexation. The crown ethers are usually used as extractants for the separation of heavy metal ions from the nuclear waste.[1] The stability of ion complexed crown ether has been well demonstrated by using the experimental techniques such as nuclear magnetic resonance,[2] calorimetric,[3] and conductometric study.[4] However, the stability may vary due to the solvent polarity and size of the ion.[2−4]

Various molecular simulation and experimental studies were reported on macrocyclic crown ethers previously[5−13] in order to understand their complexation behavior with metal ions such as Cs^+, K^+, and Li^+. The crown ether which is widely investigated using molecular simulation is 18C6.[5,6] Another macro cyclic crown ether dibenzo crown (DB18C6) or DBCE is known to display strong binding affinities for earth and alkaline metal ions.[14−16] The combined experimental and theoretical gas phase simulation studies have shown that hydronium ion strongly binds in the cavity of DBCE in the presence of organic solvents such as nitrobenzene and dichloro methane.[17] It was also experimentally proven that the presence of organic solvents such as nitromethane and acetonitrile would lead to the significant complexation of UO_2^{2+}, Ba^{2+}, Pb^{2+}, and Cd^{2+} ions with 18C6 and dicyclohexyl-18-crown-6 (DCH18C6).[18] A recent UV/vis spectroscopy study reported that the polymer supported crown ether would give thermodynamically stronger complexation compared to the crown ether without polymer.[19]

Kim et al.[20] have demonstrated that introducing crown ethers into the solution containing lanthanides leads to the complexation of metal ions with the crown ethers. Gadolinium was shown to form complexation with DBCE in the presence of nitrobenzene organic solvent using gas phase simulations.[21] Further, it was also confirmed that Gd^{3+} ions significantly bind with the polystyrene grafted crown ether.[21,22] Similarly,

Received: November 18, 2017
Revised: December 27, 2017
Published: December 27, 2017

Downloaded via INDIAN INST OF TECH KANPUR on September 24, 2021 at 07:22:02 (UTC).
See https://pubs.acs.org/sharingguidelines for options on how to legitimately share published articles.

 © 2017 American Chemical Society

DOI: 10.1021/acs.jpcb.7b11384
J. Phys. Chem. B 2018, 122, 1334−1344

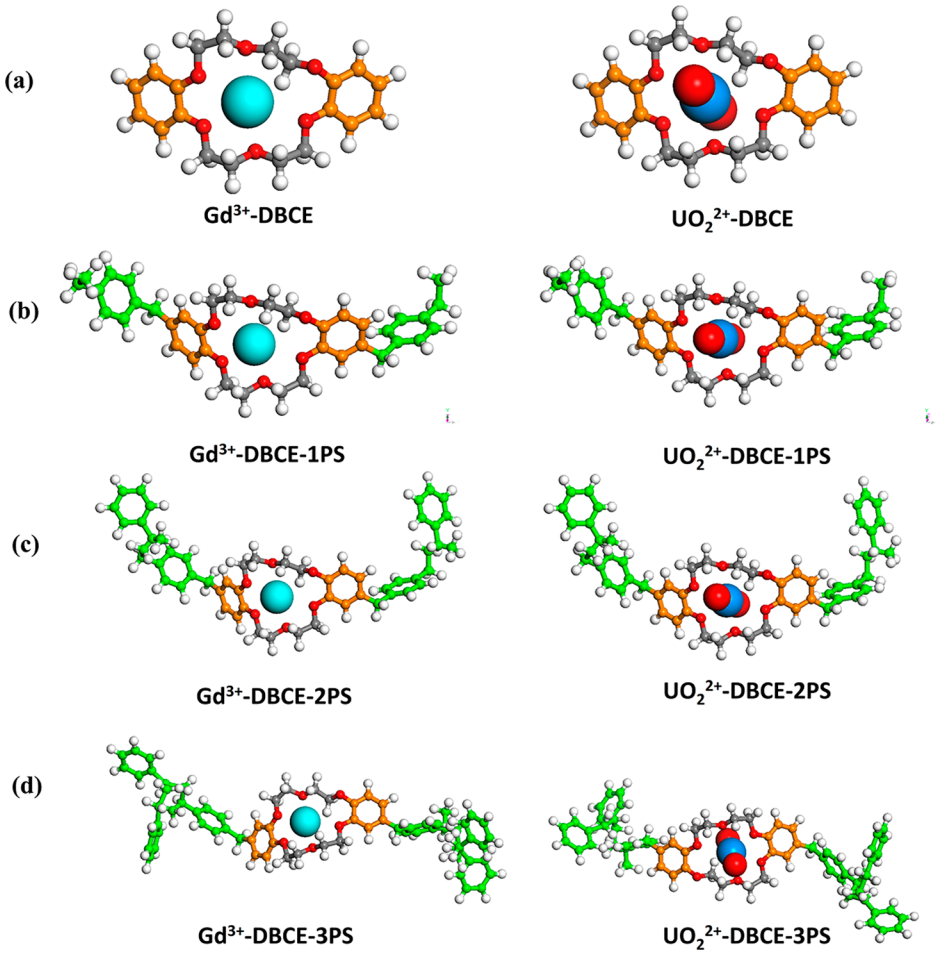

Figure 1. Schematic representation of ion complexed crown ethers with (a) DBCE, (b) DBCE-1PS, (c) DBCE-2PS, and (d) DBCE-3PS. Color codes: gray - carbon, white - hydrogen, red - oxygen, orange - benzene, green - polystyrene, cyan - gadolinium, and blue - uranium.

extraction of uranyl ions via 18C6 crown ether molecules is studied experimentally using the spectroscopic method[23] and molecular dynamics (MD) simulations.[24,25] It was reported that the utilization of nonpolar solvents favors the complexation of uranyl with the oxygens of crown ethers.[23]

Despite the above studies, not much is known about the complexation behavior of these metal ions with polymer supported crown ethers. There are many questions to be answered such as how the polystyrene grafting with DBCE influences the binding of Gd^{3+} and UO_2^{2+} in the cavity of DBCE. How the thermodynamics of metal ion binding onto the DBCE or polystyrene grafted DBCE in organic solvents affects the separation efficiency of metal ions using liquid–liquid extraction process. These questions remain unaddressed, which may play a vital role in the selectivity of DBCE toward Gd^{3+} and UO_2^{2+} and others in the solution. The aim of this study is to estimate the binding of Gd^{3+} and UO_2^{2+} with the dibenzo crown ether (DB18C6 or DBCE) using MD simulation. Further, this study investigates the effect of polystyrene (PS) grafting onto the dibenzo crown ether (DBCE-PS) in the organic solvents such as nitrobenzene (NB) and octanol (OCT).

2. METHODOLOGY AND SIMULATION DETAILS

In this work, four crown ethers were considered, viz., (1) dibenzo crown ether (DBCE or DB18C6), (2) one polystyrene on the two sides of dibenzo crown ether (DBCE-1PS), (3) two polystyrene on the two sides of dibenzo crown ether (DBCE-2PS), and (4) three polystyrene on the two sides of dibenzo crown ether (DBCE-3PS). These crown ethers were modeled using Materials Studio Visualizer interface.[26] Density functional theory (DFT) calculations at the level of B3LYP/6-31G(d,p)[27] were employed in this study to perform charge calculation and geometry optimization of DBCE, DBCE-1PS, DBCE-2PS, and DBCE-3PS structures. The optimized structures were used to prepare the initial structures for MD simulations. The initial structures for MD simulations were prepared by placing the metal ions, Gd^{3+} and UO_2^{2+}, in the cavity of crown ethers. Figure 1 displays the initial structures of DBCE, DBCE-1PS, DBCE-2PS, and DBCE-3PS. The partial charges for DBCE were taken from Peter et al.[25] On the other hand, the charges of DBCE-1PS, DBCE-2PS, and DBCE-3PS structures were derived using the CHelpG scheme as implemented in Gaussian 09 on the optimized structures. The charges for all of the structures are reported in Table S1 (Supporting Information). OPLS AA force field[28] parameters were used to account for the interactions of atoms in the crown ether, nitrobenzene,[16] octanol,[29] Gd^{3+}, NO_3^{-1},[30] and UO_2^{2+} ions.[25] Water molecules were modeled using the TIP4P model.[31] The force field parameters used to perform simulations are provided in Tables S2–S4. A cutoff radius of 1.4 nm is used for the nonbonded interactions. The calculation of electrostatics interactions was performed using the particle mesh Ewald (PME)[32] method with a cutoff of 1 nm, grid spacing of 0.1 nm, and interpolation

DOI: 10.1021/acs.jpcb.7b11384
J. Phys. Chem. B 2018, 122, 1334–1344

order of 4. All potential energy minimization calculations and MD simulations were performed using GROMACS (version 4.5.5).[33] Water geometry was constrained using the SETTLE algorithm.[34] Lennard-Jones interactions were truncated and shifted at 0.9 nm. Bond lengths were held constant using the LINCS procedure.[35] The equations of motion were integrated using the leapfrog algorithm with a time step of 2 fs. Temperature and pressure were maintained at 300 K and 1 atm, respectively, using a Berendsen thermostat and barostat.[36,37]

First, separate simulations were performed for 0.2 M $Gd(NO_3)_3$ and $UO_2(NO_3)_2$ in water, NB, and OCT. The simulations were performed such that first all of the solvent molecules were equilibrated to match the experimental density of solvents. The Gd^{3+} and UO_2^{2+} complexed crown ether molecules were randomly placed in each of the equilibrated solvents. (i.e., water, NB, and OCT). The NO_3^- counterions were added to the simulation box in order to maintain the charge neutrality. The solvated system was subjected to energy minimization without any constraints using the steepest descent method. We performed a 100 ps NVT ensemble simulation followed by a 100 ps NPT ensemble simulation, with no constraints on the water and solvent molecules, to attain a system with equilibrium temperature and pressure. This was then followed by NPT ensemble MD simulation for 20 ns, and the data was recorded at every 500 steps. The final 5 ns trajectories were used for the analysis.

We have calculated the solvation enthalpy using the relation given in eq 1. The solvation enthalpy of crown ether was calculated using the difference between the total enthalpy of the solution and that of the solvent and the vacuum.[38] In the present study, solvation enthalpy was calculated using the basic relation given as

$$\Delta H_{\text{solvation}} = H_{\text{solution}} - (H_{\text{solvent}} + H_{\text{isolated solute}}) \tag{1}$$

From the simulations, the average of the total energy was taken over 5 ns of sampling time for the solvated solute system (i.e., solvent + DBCE) and the reference systems (solvent in NPT and isolated crown ether in the vacuum).

The calculation of the binding free energy of metal ion to the ligand grafted crown ether was performed by growing the metal ions in the cavity of crown ether in the organic solvents such as NB and OCT. The free energy change is estimated by the thermodynamic integration (TI) method. In this method, we use a coupling parameter, lambda (λ), which is used to modulate the potential energy (U). U is the potential component of the Hamiltonian, which is a linear function of λ as given by the relation

$$U(\lambda) = \lambda U_1 + (1 - \lambda)U_0 \tag{2}$$

In the above equation, the coupling parameter λ represents the relation between the two states of the system, where $\lambda = 0$ initial state (no ion in the cavity of DBCE) and $\lambda = 1$ final state (fully grown ion in the cavity of DBCE). In eq 2, U_1 and U_0 are the configurational energies of the final and initial states, respectively. We have parametrized only the nonbonded interactions between guest (i.e., ion) and host (i.e., DBCE in a solvent) molecules using the coupling parameter λ. Thus, the total potential term is given similar to the study of Shirts et al.[39]

$$U(\lambda_C, \lambda_{LJ}) = U_{\text{Ion}} + U_{\text{DBCE}} + U_{\text{solvent-solvent}} + U_{\text{Ion-(DBCE+solvent)}}(\lambda_C, \lambda_{LJ}) \tag{3}$$

The λ dependent nonbonded interaction energy $U_{\text{ion-(DBCE+solvent)}}$ is defined as

$$U_{\text{ion-(DBCE+solvent)}}(\lambda_C, \lambda_{LJ}) = \sum_i \sum_{j \neq i} \left\{ \lambda_{LJ}{}^4 4\varepsilon_{ij} \left(\frac{1}{[\alpha_{LJ}(1-\lambda_{LJ})^2 + (r_{ij}/\sigma_{ij})^6]^2} - \frac{1}{[\alpha_{LJ}(1-\lambda_{LJ})^2 + (r_{ij}/\sigma_{ij})^6]} \right) + \lambda_C \frac{1}{4\pi\varepsilon_0} \frac{q_i q_j}{r_{ij}} \right\} \tag{4}$$

where α_{LJ} is the soft-core interaction potential which controls the transformation of decoupled state to fully coupled state and vice versa. λ_C and λ_{LJ} are coupling constants used for coupling of nonbonded parameters, Coulomb and van der Waals, respectively. In order to calculate the free-energy change, we have considered a two-stage thermodynamic integration method. In the first stage (ΔG_{LJ}), we take the system from an initial state, with $\lambda_{LJ} = 0$ and $\lambda_C = 0$, to the state where LJ interaction is full but with no electrostatic interaction, i.e., $\lambda_{LJ} = 1$ and $\lambda_C = 0$. In the next stage (ΔG_C), we follow a thermodynamic path where we grow the Coulombic interaction until it is full, i.e., $\lambda_{LJ} = 1$ and $\lambda_C = 1$. Thus, the total binding free-energy $\Delta G_{\text{Binding}}$ change using the two-stage TI method is given as

$$\Delta G_{\text{Binding}} = \Delta G_{LJ} + \Delta G_C \tag{5}$$

This two-stage thermodynamic integration can be expanded as

$$\Delta G_{\text{Binding}} = \int_{\lambda_{LJ}=0,\lambda_C=0}^{\lambda_{LJ}=1,\lambda_C=0} \left\langle \frac{\partial U(\lambda)}{\partial \lambda} \right\rangle_\lambda d\lambda + \int_{\lambda_{LJ}=1,\lambda_C=0}^{\lambda_{LJ}=1,\lambda_C=1} \left\langle \frac{\partial U(\lambda)}{\partial \lambda} \right\rangle_\lambda d\lambda \tag{6}$$

In order to perform MD simulation, we first compute the $\langle \partial U/\partial \lambda \rangle$ at a number of different values of λ. The values for λ_C and λ_{LJ} were varied between 0 and 1.0 in steps of 0.05. For each value of λ (21 for λ_C and 21 for λ_{LJ}), a total of 42 simulations were performed for 1 ns equilibration time followed by 5 ns simulation time for data collection.

The transfer free energy associated with the metal ion transfer from the aqueous phase to the organic phase by ion binding in the cavity of crown ether was evaluated by using the relation

$$\Delta G_{\text{Tranfer}} = \Delta G_{\text{Binding}} - \Delta G_{\text{Hydration}} \tag{7}$$

The hydration free energy ($\Delta G_{\text{Hydration}}$) was calculated by performing solvation free-energy calculations of metal ion (i.e., Gd^{3+} and UO_2^{2+}) in aqueous solution. Figure 2 shows a schematic representation of the thermodynamic cycle for the calculation of the transfer free energy of metal ion from the aqueous solution to the organic solution by complexation with DBCE as a ligand.

The self-diffusion coefficient was calculated by using the Einstein relation given as

$$D_A = \frac{1}{6t} \lim_{t\to\infty} \langle \| r_i(t) - r_i(0) \|^2 \rangle_{i \in A} \tag{8}$$

where D_A is self-diffusion coefficient of molecular species A and $r_i(t)$ is the center-of-mass position vector of a molecule at time t.

DOI: 10.1021/acs.jpcb.7b11384
J. Phys. Chem. B 2018, 122, 1334−1344

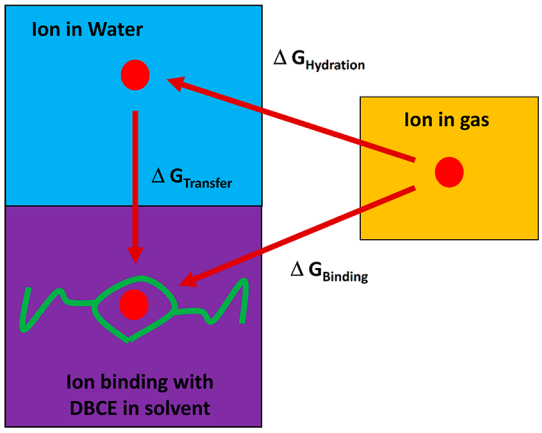

Figure 2. Schematic representation of the thermodynamic cycle for calculating transfer free energy ($\Delta G_{Transfer}$). $\Delta G_{Hydration}$ is the hydration free energy of metal ion in water, and $\Delta G_{Binding}$ is the binding free energy of metal ion to the crown ether in the presence of organic solvent.

3. RESULTS AND DISCUSSION

3.1. $Gd(NO_3)_3$ and $UO_2(NO_3)_2$ Structural Properties. We first studied the structural properties of Gd^{3+} and UO_2^{2+} in different solvents in order to ascertain the quality of the force field used in this work by comparing with the existing literature. The radial distribution function (RDF) plot for the Gd^{3+}–water structure is presented in Figure S1a and b. The first peak position for the Gd^{3+}–water oxygen (O_W) and Gd^{3+}–water hydrogen (H_W) are located at ∼0.24 and ∼0.31 nm, respectively, which are in excellent agreement with previous diffraction and X-ray adsorption fine structure experiments.[40] The obtained value for the first peak location is also in agreement with electron resonance experiments.[41,42] Furthermore, our results are akin to that of ab initio MD simulations, which reported 0.237 and 0.31 nm as the first peak of Gd^{3+}–O_W and Gd^{3+}–H_W, respectively[43,44] The coordination number for Gd^{3+}–O_W is ∼2.6, while for Gd^{3+}–H_W it is 5.2. These values are in agreement with the results of a previous simulation study.[44] The second coordination shell also exists due to significant electrostatic interactions with peaks located at 0.44 nm for Gd^{3+}–O_w and 0.51 nm for Gd^{3+}–H_W. These values are also in agreement with the previous simulations.[44]

Figure S1c and d presents the RDF plots of Gd^{3+}–octanol. The first peak is located at 0.24 nm for the Gd^{3+}–octanol oxygen (O_{OCT}). On the other hand, the first peak for the Gd^{3+}–octanol hydrogen (H_{OCT}) is located at 0.29 nm. The RDF plot of Gd^{3+}–nitrobenzene is shown in Figure S1e and f. The first peak of the RDF plot for the Gd^{3+}–oxygen's of nitrobenzene (O_{NB}) is located at 0.27 nm, and for the Gd^{3+}–nitrogen of nitrobenzene (N_{NB}), the first peak is located at 0.38 nm. Unfortunately, no experimental data is available for these systems, to the best of our knowledge. Nonetheless, our results

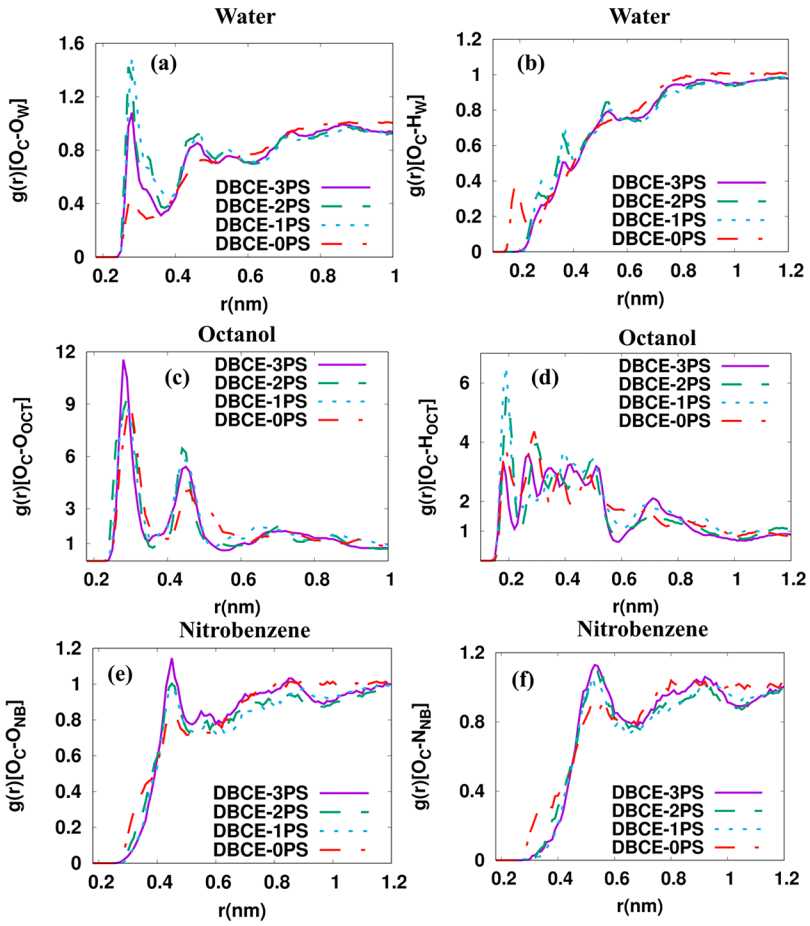

Figure 3. RDF plot of oxygens of crown ether (O_C) with solvent molecules for Gd^{3+} complexed DBCE: (a) O_C–OW, (b) O_C–HW, (c) O_C–O_{OCT}, (d) O_C–H_{OCT}, (e) O_C–O_{NB}, and (f) O_C–N_{NB}.

DOI: 10.1021/acs.jpcb.7b11384
J. Phys. Chem. B 2018, 122, 1334−1344

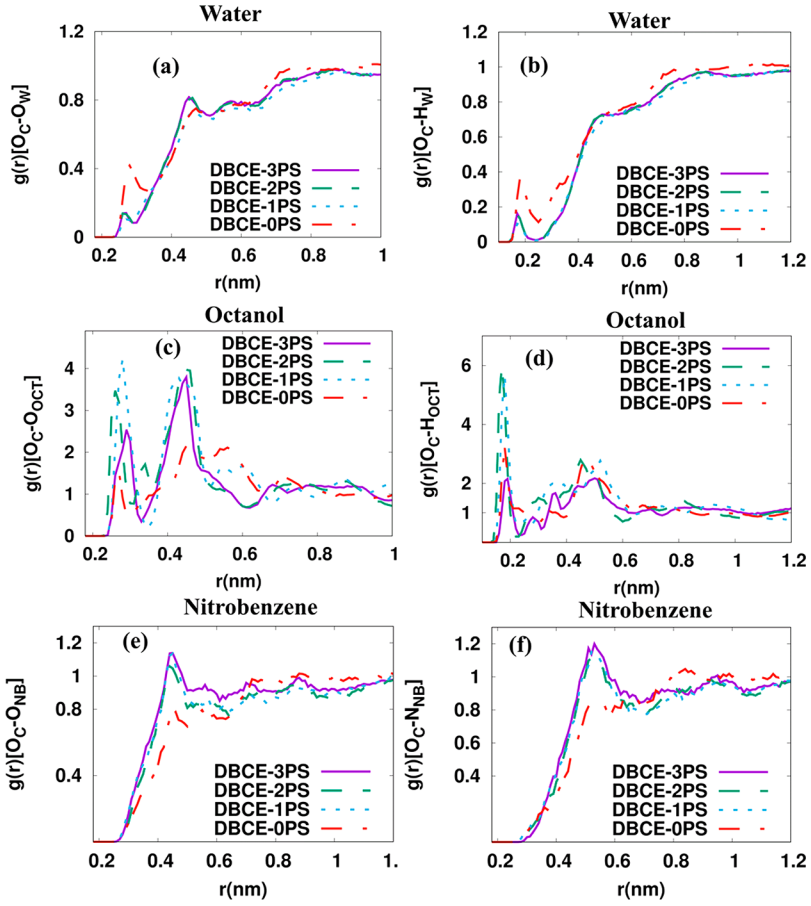

Figure 4. RDF plot of oxygens of crown ether (O_C) with solvent molecules for UO_2^{2+} complexed DBCE: (a) O_C−OW, (b) O_C−HW, (c) O_C−O_{OCT}, (d) O_C−H_{OCT}, (e) O_C−O_{NB}, and (f) O_C−N_{NB}.

are in agreement with the DFT simulation study on a series of lanthanides (Ln^{3+})[45] with a reported value of 0.24 nm as the first peak for the Ln^{3+}−O.

Figure S2 reports the RDF plots of UO_2^{2+} with water, OCT, and NB. The first peak locations for the U_{UO2}−O_W, U_{UO2}−O_{OCT}, and U_{UO2}−O_{NB} are 0.24, 0.24, and 0.27 nm, respectively. Similarly, the first peaks for the RDFs of U_{UO2}−H_W, U_{UO2}−H_{OCT}, and U_{UO2}−N_{NB} are located at 0.31, 0.29, and 0.38 nm, respectively. The peak locations observed in our simulation are well in agreement with a previous MD simulation study.[24] Furthermore, the results are also in agreement with the experimental NMR and X-ray diffraction studies for U_{UO2}−O_W.[47,48] However, no experimental data are available for either Gd^{3+} or UO_2^{2+} in organic solvents. We also investigated the RDFs of NO_3^-−solvent, Gd^{3+}−NO_3^-, and UO_2^{2+}−NO_3^- (see Figures S3−S5 in the Supporting Information), and the results are in agreement with the previous simulations.[46] In the next section, we describe the structure and solvation properties of DBCE with grafted PS in water and in organic solvents, viz., NB and OCT.

3.2. Structure and Solvation Properties of Gd^{3+}−DBCE and UO_2^{2+}−DBCE. Figure 3 presents the RDF of Gd^{3+} complexed DBCE, DBCE-1PS, DBCE-2PS, and DBCE-3PS in water, octanol, and nitrobenzene. The RDF is evaluated between oxygens of crown ether (O_C) and oxygen and hydrogens of solvent molecules. The first peak for the pair of O_C−O_W is located at 0.28 nm, and for O_C−H_W, it is located at 0.18 nm. The effect of PS monomers is reflected in the coordination numbers between DBCE−water which show a decrease from 4 to 2 for O_C−O_W and 1.5 to 0.7 for O_C−H_W with an increase in PS chain length from DBCE to DBCE-3PS. This indicates that an increase in the polystyrene chain length would lead to the unfavorable interactions of DBCE with water molecules. The RDF analysis of crown ether (18C6) with water molecules (O_C−O_W) shows the location of the first salvation shell in the range 0.277−0.29 nm. Furthermore, the water coordination numbers vary in the range 2−3.[49]

Similarly, the RDF between DBCE and OCT shows a first coordination shell at ∼0.28 nm for O_C−O_{OCT} and ∼0.19 nm for O_C−H_{OCT}. The coordination numbers show a slight decrease from 3 to 2 for O_C−O_{OCT} and 0.4−0.2 for O_C−H_{OCT} in going from DBCE to DBCE-3PS. The RDF of DBCE and NB shows the first coordination shell at 0.45 nm for O_C−O_{NB} and 0.51 nm for O_C−N_{NB}. The corresponding coordination numbers show almost similar values: ∼3.3 for O_C−O_{NB} and ∼3.1 for O_C−N_{NB}.

Figure 4 presents RDFs between UO_2^{2+} complexed DBCE in water, NB, and OCT which are akin to that seen in Figure 3. However, the results have not shown any significant difference by complexing with Gd^{3+} and UO_2^{2+} ions to DBCE in the presence of NB and OCT solvents. It is observed that O_C−O_{NB} and O_C−O_{OCT} RDF peak intensity and coordination numbers do not differ much in going from DBCE to DBCE-3PS in the organic solvents. Table 1 summarizes all of the coordination numbers obtained for different cases as discussed above.

The calculated values of the various enthalpies of solvation are presented in Figure 5. It is observed that hydration enthalpies for both Gd^{3+} and UO_2^{2+} complexed DBCE become

DOI: 10.1021/acs.jpcb.7b11384
J. Phys. Chem. B 2018, 122, 1334−1344

Table 1. Coordination Numbers for O_C-O_W, O_C-H_W, O_C-O_{OCT}, O_C-H_{OCT}, O_C-O_{NB}, and O_C-N_{NB} Pairs[a]

	Gd $(NO_3)_3$				UO_2 $(NO_3)_2$			
pair	0PS	1PS	2PS	3PS	0PS	1PS	2PS	3PS
O_C-O_W	5.1	4.1	3.3	2.4	1.0	0.1	0.1	0.1
O_C-H_W	2.0	1.5	1.2	0.7	0.4	0.1	0.1	0.1
O_C-O_{OCT}	3.2	2.5	2.7	2.2	0.6	0.8	0.5	0.5
O_C-H_{OCT}	0.6	0.5	0.5	0.2	0.3	0.3	0.3	0.2
O_C-O_{NB}	3.3	3.5	3.3	3.4	2.0	4.3	3.2	4.1
O_C-N_{NB}	3.3	3.1	3.5	3.3	2.3	3.1	3.4	3.8

[a]The standard deviation values are within (±5−7%).

favorable in NB and OCT. It is very clear from the plots that the solvation of ion complexed DBCE becomes unfavorable (i.e., less negative with increase in PS length). The solvation of ion−DBCE becomes favorable in the organic solvents, NB and OCT (less positive in NB and more negative in OCT). It is observed that a significant solvation is seen in NB and OCT for Gd^{3+}−DBCE compared to UO_2^{2+}−DBCE. The observed solvation enthalpy values in all three solvents are in accordance with the observed structural properties. The dominant contribution comes from electrostatic interactions of ion−DBCE to solvent, as it is observed that, for the solvation enthalpy of Gd^{3+}−DBCE in water, the electrostatic contribution is -87.22×10^3 kJ/mol and the van der Waals contribution to solvation enthalpy is 1.37×10^3 kJ/mol.

3.3. Gd^{3+} and UO_2^{2+} Binding and Diffusion. Figure 6 presents the RDFs of O_C-Gd^{3+} and O_C-U_{UO2} in NB and OCT. The significant first peak for the O_C-Gd^{3+} and O_C-U_{UO2} RDFs is located at ∼0.24 nm for all of the polystyrene grafted DBCEs in nitrobenzene and octanol (see Figure 6a and b). However, for DBCE-0PS (without polystyrene grafting), no significant peak is observed. Our results are in agreement with the simulation study on a series of Ln^{3+} ions on oxygens of 18C6 which showed a peak located at 0.245 nm for $Gd^{3+}-O_C$.[30] This illustrates that the increase in polystyrene graft length increases the propensity for the ion to tightly bind within the cage.

Figure 6c and d presents the RDF plot between O_C-U_{UO2} in different solvents. The peak locations vary in the range ∼0.22−0.24 nm for all three polystyrene grafted crown ethers studied here. A very small peak is seen in the case of DBCE without polymer grafting. Our results here are in agreement with a previous simulation study by Peter et al.[29] From all of the results, it is very clear that binding of Gd^{3+} and UO_2^{2+} ions is significantly favorable for polystyrene grafted DBCE. The increase in hydrophobicity via adding the polystyrene monomers is found to enhance the binding affinity of ions.

Figure 7 presents the ion self-diffusion coefficient (D) values of Gd^{3+} and UO_2^{2+} in the presence of NB and OCT. The corresponding mean square displacement (MSD) plots are shown in Figure S6. The D values show a decrease with an increase in polystyrene monomer length. The calculated diffusion coefficient values for both Gd^{3+} and UO_2^{2+} from the current simulation study in the organic solvents OCT and NB are in the same order of magnitude as in the previous literature.[50,51] The experimentally reported self-diffusion coefficients in aqueous solution are $\sim 0.58 \times 10^{-5}$ cm^2/s for Gd^{3+} [50] and $\sim 0.43 \times 10^{-5}$ cm^2/s for UO_2^{2+}.[51] The observed D values from our simulations differ slightly due to significant binding with respect to the oxygens of crown ethers. In NB, these values are in the range $(0.4-0.1) \times 10^{-5}$ cm^2/s for Gd^{3+} and UO_2^{2+} for all four DBCE. It is also observed that there is a very slow diffusion ($\sim 10^{-8}$ cm^2/s) of Gd^{3+} and UO_2^{2+} in octanol. The observed slower diffusion of Gd^{3+} and UO_2^{2+} is due to significant binding in the presence of organic solvents (OCT and NB) compared to diffusion of these ions in aqueous solution.[50,51] Another possible reason for this slower diffusion in organic solvents compared to water could be very low solvent polarity, as the dielectric constant values for NB and OCT are 34.8 and 10.3, respectively.

3.4. Binding Free Energy. Figure 8 presents the free-energy change ($\delta U/\delta\lambda$) as a function of coupling parameter (λ) for the process of Gd^{3+} binding in the cage of DBCE. The free energy of binding of the metal ion with the crown ether is calculated by growing the metal ion in the cavity of the crown ether in the presence of organic solvents such as OCT and NB. It is evident from the plots that electrostatic contribution to the binding free energy is more favorable than that due to the dispersive van der Waals interactions. The significant minima in the free energy for Gd^{3+} is observed for DBCE-3PS in both solvents OCT and NB. Thus, the binding becomes more favorable with increasing PS chain length. Figure 9 presents $\delta U/\delta\lambda$ as a function of the coupling parameter (λ) for the UO_2^{2+} binding to DBCE, whose behavior is akin to that seen in Figure 8.

Figure 10 presents the $\Delta G_{Binding}$ of metal ion in the cavity of crown ether, calculated using eq 5. It is noted that the binding of Gd^{3+} to the crown ether is more favorable compared to UO_2^{2+} in both solvents, NB and OCT. Further, it is evident that the binding free energies for both Gd^{3+} and UO_2^{2+} in the

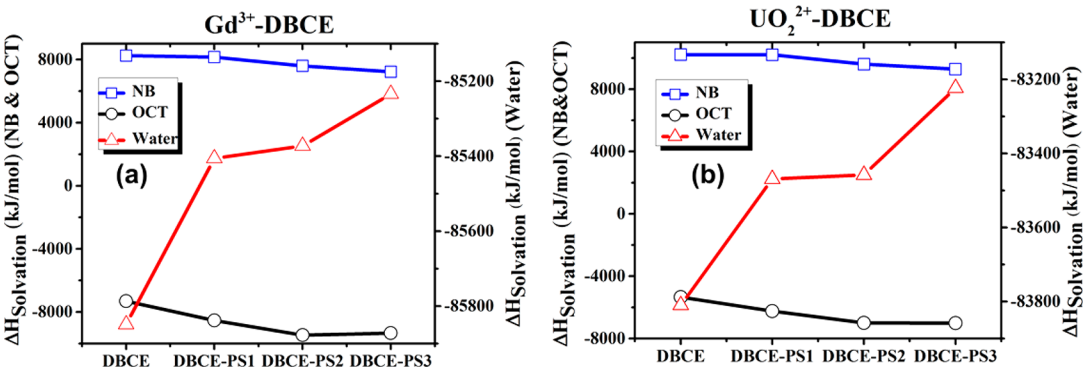

Figure 5. Solvation enthalpy of ion complexed crown ether and polystyrene grafted crown ether in different solvents: (a) Gd^{3+}−DBCE, (b) UO_2^{2+}−DBCE. The standard deviation values are within ±5%.

DOI: 10.1021/acs.jpcb.7b11384
J. Phys. Chem. B 2018, 122, 1334−1344

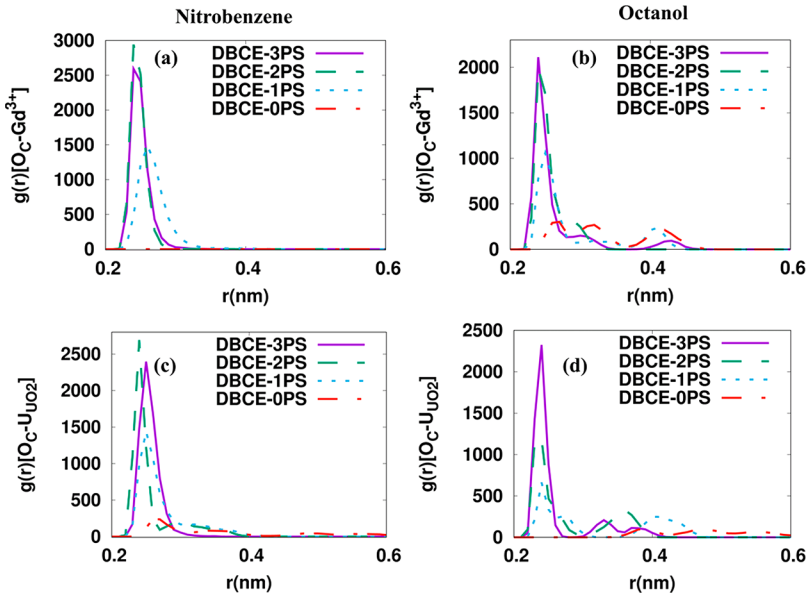

Figure 6. RDF between O_C−Gd^{3+} in the presence of (a) NB and (b) OCT. RDF between O_C−U_{UO2} in the presence of (c) NB and (d) OCT.

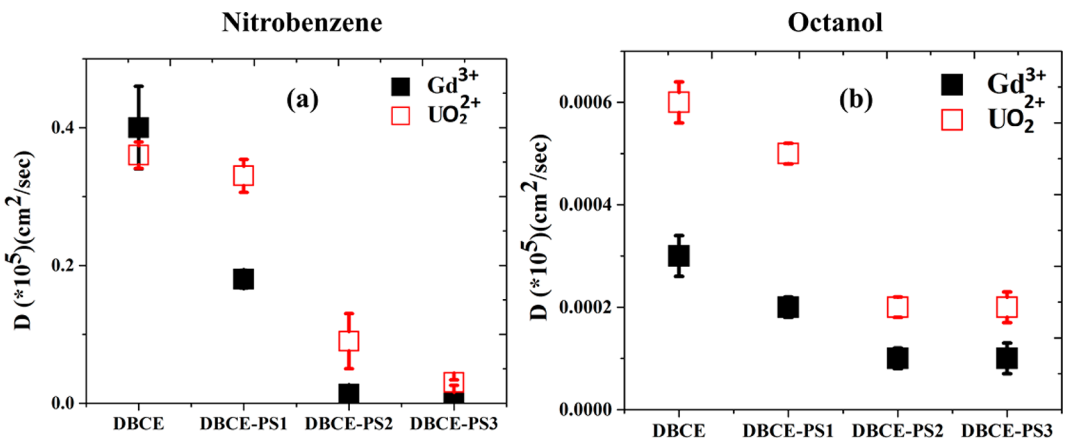

Figure 7. Diffusion coefficient (D) values of ions in organic solvents: (a) NB and (b) OCT.

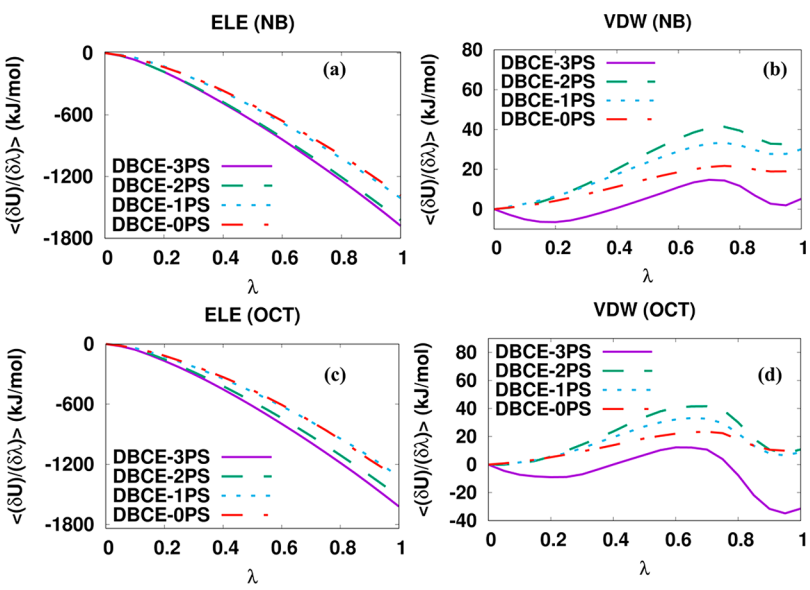

Figure 8. Electrostatic (ELE) and van der Waals (vdW) contributions to the free energy change for Gd^{3+} ion with various graft lengths of polystyrene in the presence of NB (a and b) and OCT (c and d).

DOI: 10.1021/acs.jpcb.7b11384
J. Phys. Chem. B 2018, 122, 1334−1344

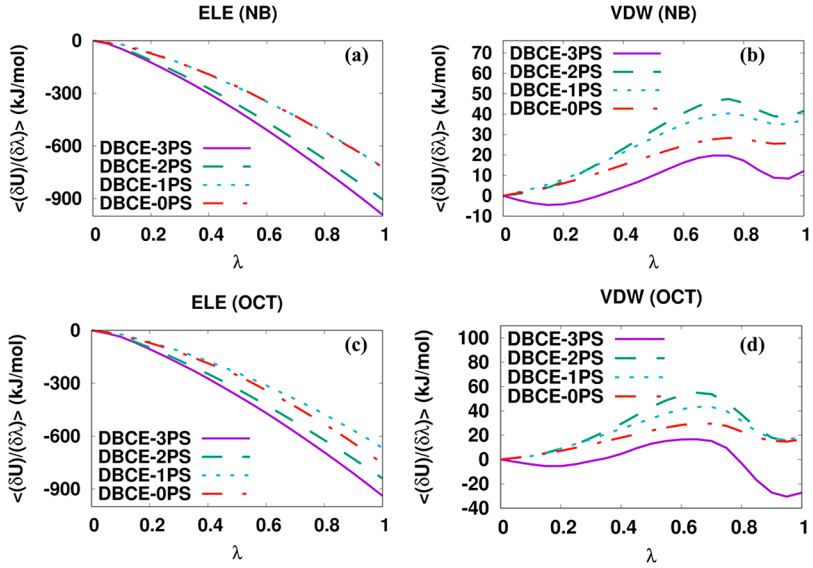

Figure 9. Electrostatic (ELE) and van der Waals (vdW) contributions to the free energy change for UO_2^{2+} ion with various graft lengths of polystyrene in the presence of NB (a and b) and OCT (c and d).

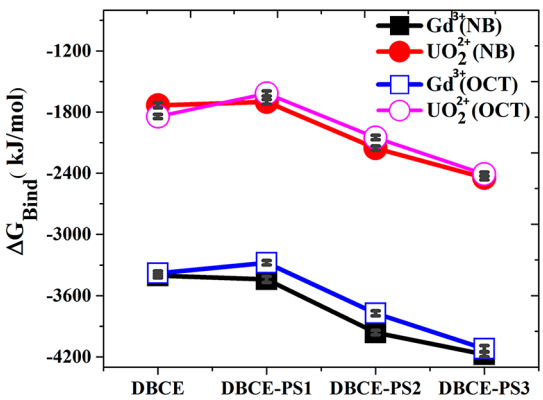

Figure 10. Binding free energy (ΔG_{Bind}) of metal ions as a function of polystyrene graft length.

cavity of DBCE-3PS are higher than those in the cavities of DBCE-2PS and DBCE-1PS and DBCE-0PS in OCT and NB. The $\Delta G_{Binding}$ values with DBCE and DBCE-1PS are comparable. However, the $\Delta G_{Binding}$ value becomes more negative (i.e., more favorable) with further increase in polystyrene grafting. The favorable binding free energy of metal ions within the cavity of crown ethers follows the order: DBCE-3PS > DBCE-2PS > DBCE-1PS > DBCE-0PS. Overall, it is observed that with an increase in grafting of polystyrene the $\Delta G_{Binding}$ becomes more favorable for Gd^{3+} and UO_2^{2+}. However, it is also observed that $\Delta G_{Binding}$ (NB) > $\Delta G_{Binding}$ (OCT) for both Gd^{3+} and UO_2^{2+}. The only available binding energy of Gd with EDTA as a ligand is −4424.7 kJ/mol studied by gas phase simulation study.[22] Interestingly, our current results of binding free energy for Gd^{3+} are in the same order of magnitude. There was no literature available for qualitative or quantitative comparison of the binding free energy of UO_2^{2+}.

3.5. Transfer Free Energy and Partition Coefficient. The transfer free energy ($\Delta G_{Transfer}$) of metal ion from the water phase to the cavity of crown ether in the organic phase is useful in estimating the transferability of metal ions from one phase to another phase. This is particularly used in separation or extraction of the metal ions from an aqueous phase to an organic phase via complexation to ligands.[52,53] The observed hydration free energy $\Delta G_{Hydration}$ is −2897.6 ± 3.6 kJ/mol for Gd^{3+} and −1274.6 ± 1.9 kJ/mol for UO_2^{2+}. The calculated $\Delta G_{Hydration}$ is in good agreement with previous simulation studies reported as −3429.2 kJ/mol for Gd^{3+} [30] and −1267.7 kJ/mol for UO_2^{2+}.[24] The experimentally reported hydration free energy for Gd^{3+} [30] is −3372.3 kJ/mol, and that for UO_2^{2+} [24] is −1330.2 kJ/mol.

Figure 11 displays the transfer free energy $\Delta G_{Transfer}$ of metal ion calculated using eq 7 for both Gd^{3+} and UO_2^{2+}. It is observed that $\Delta G_{Tranfer}$ of metal ions Gd^{3+} and UO_2^{2+} becomes more negative (i.e., more favorable) with an increase in the grafting density of polystyrene on the crown ether. The free energy is more negative for the transfer of Gd^{3+} when compared to UO_2^{2+} from aqueous solution to organic solution of NB or OCT. It is clearly evident from the figure that the transfer of Gd^{3+} with polystyrene grafted crown ether becomes significantly favorable compared to the case of UO_2^{2+}. The transfer free energy values are almost similar for the DBCE and DBCE-1PS. However, the transfer free energy becomes increasingly negative with a further increase in the grafted polystyrene chain length.

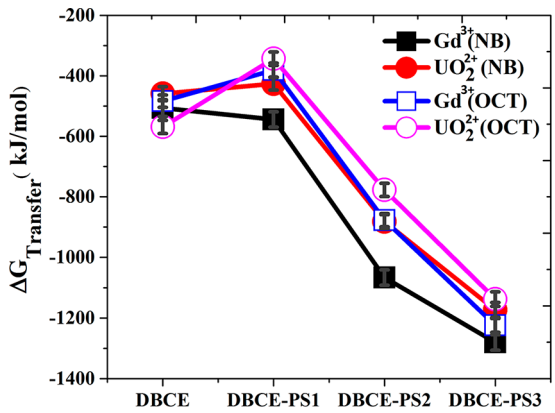

Figure 11. Transfer free energy ($\Delta G_{Transfer}$) of metal ions as a function of polystyrene graft length.

DOI: 10.1021/acs.jpcb.7b11384
J. Phys. Chem. B 2018, 122, 1334−1344

The partition coefficient (P) is an important thermodynamic quantity usually employed to understand the partitioning of solutes or ions between aqueous and organic phases. This is defined as the ratio of the concentration of solutes/ions in the organic phase to an aqueous phase, generally represented as log P. This also can be expressed as[52]

$$\log P = \frac{\Delta G_{\text{Binding}} - \Delta G_{\text{Hydration}}}{2.303RT} \quad (9)$$

where $\Delta G_{\text{Binding}}$ is the Gibbs free energy of binding of the ion to the crown ether in the organic phase and $\Delta G_{\text{Hydration}}$ is the hydration free energy of ion at a given temperature and pressure.

Figure 12 presents the partition coefficient values of metal ions. The calculated partition coefficient values vary in the range ∼88−222 for Gd^{3+} and ∼79−200 for UO_2^{2+} with an increase in polystyrene chain length. It is noted that the partition function for alkane molecules in the water−octanol system is in the range 1−7.[53] The previous simulation studies have reported partition coefficient values in the range ∼1−23 for Ba^{2+} and Sr^{2+} metal ions in different aqueous−organic phases with organic solvents such as carbon tetrachloride (CCl_4), propane (C_3H_8), etc.[54] However, significantly higher values of log P values are observed for both Gd^{3+} and UO_2^{2+} between the aqueous to solvent phase. The larger value of log P values reported here is indicative of a stronger tendency of partitioning of metal ions with the organic phase via complexation with DBCE molecules. An increase of polystyrene chain length on the DBCE is found to be favorable for the ion complexation. It is also observed that partition of Gd^{3+} molecules is higher than that for UO_2^{2+}, which is in agreement with the observed values of binding free energy. From these results, it is also very clear that both NB and OCT are favorable for the transfer of Gd^{3+} and less favorable for UO_2^{2+} via complexing with the polystyrene grafted crown ether. The ion partitioning is significant particularly when crown ether is grafted with three monomers of polystyrene, grafted on either side (i.e., DBCE-3PS).

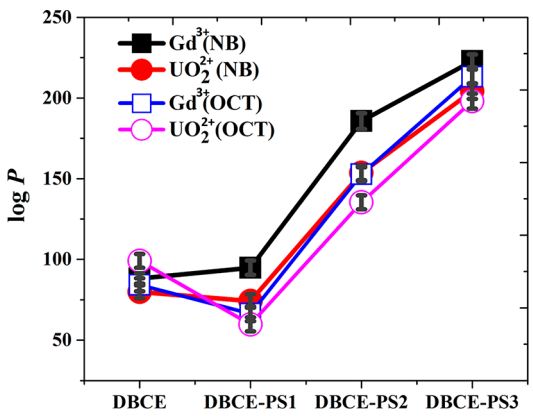

Figure 12. Partition coefficient (log P) of metal ions as a function of polystyrene graft length.

4. CONCLUSIONS

In this Article, Gd^{3+} and UO_2^{2+} metal ion complexation with dibenzo crown ether (DBCE) is studied using all-atom molecular dynamic simulations. In particular, the role of polystyrene grafting on dibenzo crown ether (DBCE-PS) is investigated on the complexation of metal ions to the crown ethers in the organic solvents, nitrobenzene and octanol. The structural arrangement of Gd^{3+} and UO_2^{2+} ions in solvent molecules is found to be in good agreement with the available experimental literature and previous simulation studies. The ion self-diffusion coefficient of Gd^{3+} and UO_2^{2+} is found to be significantly lower, due to strong binding of ions with the crown ether.

The calculated $\Delta G_{\text{Binding}}$ of metal ion onto the crown ether becomes 2-fold more negative (i.e., more favorable) for Gd^{3+} and UO_2^{2+} with an increase in the graft length of polystyrene. On the basis of the binding free-energy calculations, it was observed that binding of Gd^{3+} to crown ether is more favorable, compared to the case of UO_2^{2+}, in both of the solvents NB and OCT. Favorable $\Delta G_{\text{Binding}}$ of Gd^{3+} and UO_2^{2+} ions within the cavity of crown ethers is found to follow the order DBCE-3PS > DBCE-2PS > DBCE-1PS > DBCE-0PS. $\Delta G_{\text{Transfer}}$ of metal ions Gd^{3+} and UO_2^{2+} becomes more negative (i.e., more favorable) with an increase in the graft length of polystyrene on the crown ether. The higher separation is seen for DBCE-3PS. The calculated partition coefficient (log P) values vary in the range ∼88−222 for Gd^{3+} and ∼79−200 for UO_2^{2+} with increasing polystyrene grafting. The higher log P values show higher separation of metal ions from an aqueous phase to a solvent phase. The partition of Gd^{3+} molecules is slightly higher compared to UO_2^{2+}, which is in agreement with observed values of $\Delta G_{\text{Binding}}$. On the basis of the observations of $\Delta G_{\text{Transfer}}$ and log P, the organic solvents such as NB and OCT, with DBCE-3PS, would be favorable candidates for the $Gd^{3+}$and UO_2^{2+} crown ether binding, and thus can be used for the separation of these ions from an aqueous phase.

■ ASSOCIATED CONTENT

Supporting Information

The Supporting Information is available free of charge on the ACS Publications website at DOI: 10.1021/acs.jpcb.7b11384.

Partial atomic charges, potential parameters, and Gd-$(NO_3)_3$ and $UO_2(NO_3)_2$ structural details (PDF)

■ AUTHOR INFORMATION

Corresponding Authors

*E-mail: musharaf@barc.gov.in.

*Phone: 91-512-259 6141 (office). Fax: 91-512-259 0104. E-mail: jayantks[AT]iitk.ac.in.

ORCID

Sk. Musharaf Ali: 0000-0003-0457-0580

Jayant Kumar Singh: 0000-0001-8056-2115

Notes

The authors declare no competing financial interest.

■ ACKNOWLEDGMENTS

This work is supported by Board of Research on Nuclear Sciences (BRNS), Department of Atomic Energy (DAE), and Government of India, sanctioned no: 36(1)/14/02/2015-BRNS/100. We are grateful to HPC, IIT Kanpur, for the computational support. P.S. gratefully acknowledges Science and Engineering Research Board (SERB) for the National Post-Doctoral Fellowship (PDF/2017/000121).

REFERENCES

(1) Alp, H.; Gök, H. Z.; Kantekin, H.; Ocak, Ü. Synthesis and metal ion binding properties of thiaaza crown macrocycles. *J. Hazard. Mater.* **2008**, *159*, 519−522.

(2) Karkhaneei, E.; Zebarjadian, M. H.; Shamsipur, M. Complexation of Ba2+, Pb2+, Cd2+, and UO22+ Ions with 18-Crown-6 and Dicyclohexyl-18-Crown-6 in Nitromethane and Acetonitrile Solutions by a Competitive NMR Technique Using the 7Li Nucleus as a Probe. *J. Solution Chem.* **2001**, *30*, 323−333.

(3) Buschmann, H. J. A comparison of different experimental techniques for the determination of the stabilities of polyether, crown ether and cryptand complexes in solution. *Inorg. Chim. Acta* **1992**, *195*, 51−60.

(4) Buschmann, H. J.; Mutihac, R. C.; Schollmeyer, E. Interactions between crown ethers and water, methanol, acetone, and acetonitrile in halogenated solvents. *J. Solution Chem.* **2010**, *39*, 291−299.

(5) Ranghino, G.; Romans, S.; Lehn, J. M.; Wipff, G. Monte Carlo study of the conformation-dependent hydration of the 18-crown-6 macrocycle. *J. Am. Chem. Soc.* **1985**, *107*, 7873−7877.

(6) Dang, L. X. Free energies for association of Cs+ to 18-crown-6 in water. A molecular dynamics study including counter ions. *Chem. Phys. Lett.* **1994**, *227*, 211−214.

(7) Van Eerden, J.; Harkema, S.; Feil, D. Molecular dynamics of 18-crown-6 complexes with alkali-metal cations: calculation of relative free energies of complexation. *J. Phys. Chem.* **1988**, *92*, 5076−5079.

(8) Troxler, L.; Wipff, G. Conformation and dynamics of 18-crown-6, cryptand 222, and their cation complexes in acetonitrile studied by molecular dynamics simulations. *J. Am. Chem. Soc.* **1994**, *116*, 1468−1480.

(9) Chaumont, A.; Schurhammer, R.; Vayssière, P.; Wipff, G. Simulations of the Dynamics of 18-Crown-6 and its Complexes: From the Gas Phase to Aqueous Interfaces with SC-CO 2 and a Room-Temperature Ionic Liquid. *Macrocyclic. Chem.* **2005**, 327−348.

(10) Dang, L. X.; Kollman, P. A. Free energy of association of the 18-crown-6: K+ complex in water: a molecular dynamics simulation. *J. Am. Chem. Soc.* **1990**, *112*, 5716−5720.

(11) Krongsuk, S.; Kerdcharoen, T.; Hannongbua, S. How many water molecules in the hydration shell of 18-crown-6? Monte Carlo simulations based on ab initio-derived potential energy surface. *J. Phys. Chem. B* **2003**, *107*, 4175−4181.

(12) Kowall, T.; Geiger, A. Molecular Dynamics Simulation Study of 18-Crown-6 in Aqueous Solution. 2. Free Energy Profile for the Association 18C6. cntdot.. cntdot.. cntdot. K+ in Water. *J. Phys. Chem.* **1995**, *99*, 5240−5246.

(13) Sun, Y.; Kollman, P. A. Conformational sampling and ensemble generation by molecular dynamics simulations: 18-Crown-6 as a test case. *J. Comput. Chem.* **1992**, *13*, 33−40.

(14) Pedersen, C. J.; Frensdorff, H. K. MakrocyclischePolyäther und ihreKomplexe. *Angew. Chem.* **1972**, *84*, 16−26.

(15) Pedersen, C. J. Cyclic polyethers and their complexes with metal salts. *J. Am. Chem. Soc.* **1967**, *89*, 7017−7036.

(16) Sahu, P.; Ali, S. M.; Singh, J. K. Structural and dynamical properties of Li+-dibenzo-18-crown-6 (DB18C6) complex in pure solvents and at the aqueous-organic interface. *J. Mol. Model.* **2014**, *20*, 2413.

(17) Kříž, J.; Dybal, J.; Makrlík, E.; Budka, J. Interaction of hydronium ion with dibenzo-18-crown-6: NMR, IR, and theoretical study. *J. Phys. Chem. A* **2008**, *112*, 10236−10243.

(18) Karkhaneei, E.; Zebarjadian, M. H.; Shamsipur, M. Complexation of Ba2+, Pb2+, Cd2+, and UO22+ Ions with 18-Crown-6 and Dicyclohexyl-18-Crown-6 in Nitromethane and Acetonitrile Solutions by a Competitive NMR Technique Using the 7Li Nucleus as a Probe. *J. Solution Chem.* **2001**, *30*, 323−333.

(19) Bey, A.; Dreyer, O.; Abetz, V. Thermodynamic analysis of alkali metal complex formation of polymer-bonded crown ether. *Phys. Chem. Chem. Phys.* **2017**, *19*, 15924.

(20) Kim, H. S.; Chi, K. W. Monte Carlo simulation study for QSPR of solvent effect on the selectivity of 18-crown-6 between Gd 3+ and Yb 3+ ions. *J. Mol. Struct.: THEOCHEM* **2005**, *722*, 1−7.

(21) Boda, A.; Arora, S. K.; Deb, A. K.; Joshi, J. M.; Jha, M.; Govalkar, S.; Shenoy, K. T. Molecular Modelling Guided Experimental Study for Isotopic Enrichment of Gadolinium. *BARC Newsl.* **2015**, 6−12.

(22) Boda, A.; Arora, S. K.; Singha Deb, A. K.; Jha, M.; Ali, S. M.; Shenoy, K. T. Molecular modeling guided isotope separation of gadolinium with strong cation exchange resin using displacement chromatography. *Sep. Sci. Technol.* **2017**, *52*, 2300−2307.

(23) Eller, P. G.; Penneman, R. A. Synthesis and structure of the 1:1 uranyl nitrate tetrahydrate-18-crown-6 compound, UO2 (NO3) 2 (H2O) 2.2 H2O.(18-crown-6). Noncoordination of uranyl by the crown ether. *Inorg. Chem.* **1976**, *15*, 2439−2442.

(24) Guilbaud, P.; Wipff, G. Hydration of uranyl ($UO^{2+}{}_2$) cation and its nitrate ion and 18-crown-6 adducts studied by molecular dynamics simulations. *J. Phys. Chem.* **1993**, *97*, 5685−5692.

(25) Grootenhuis, P. D.; Kollman, P. A. Molecular mechanics and dynamics studies of crown ether-cation interactions: free energy calculations on the cation selectivity of dibenzo-18-crown-6 and dibenzo-30-crown-10. *J. Am. Chem. Soc.* **1989**, *111*, 2152−2158.

(26) *Materials Studio Modeling Environment*, release 5.0; Accelrys Software Inc.: San Diego, CA, 2007.

(27) Lee, C.; Yang, W.; Parr, R. G. Development of the Colle-Salvetti correlation-energy formula into a functional of the electron density. *Phys. Rev. B: Condens. Matter Mater. Phys.* **1988**, *37*, 785.

(28) Jorgensen, W. L.; Maxwell, D. S.; Tirado-Rives, J. Development and testing of the OPLS all-atom force field on conformational energetics and properties of organic liquids. *J. Am. Chem. Soc.* **1996**, *118*, 11225−11236.

(29) DeBolt, S. E.; Kollman, P. A. Investigation of structure, dynamics, and solvation in 1-octanol and its water-saturated solution: molecular dynamics and free-energy perturbation studies. *J. Am. Chem. Soc.* **1995**, *117*, 5316−5340.

(30) vanVeggel, F. C.; Reinhoudt, D. N. New, Accurate Lennard-Jones Parameters for Trivalent Lanthanide Ions, Tested on [18] Crown−6. *Chem. - Eur. J.* **1999**, *5*, 90−95.

(31) Abascal, J. L.; Vega, C. A general purpose model for the condensed phases of water: TIP4P/2005. *J. Chem. Phys.* **2005**, *123*, 234505.

(32) Darden, T.; York, D.; Pedersen, L. Particle mesh Ewald: An N·log (N) method for Ewald sums in large systems. *J. Chem. Phys.* **1993**, *98*, 10089−10092.

(33) Pronk, S.; Páll, S.; Schulz, R.; Larsson, P.; Bjelkmar, P.; Apostolov, R.; Hess, B. GROMACS 4.5: a high-throughput and highly parallel open source molecular simulation toolkit. *Bioinformatics* **2013**, *29*, 845−854.

(34) Miyamoto, S.; Kollman, P. A. SETTLE: an analytical version of the SHAKE and RATTLE algorithm for rigid water models. *J. Comput. Chem.* **1992**, *13*, 952−962.

(35) Hess, B.; Bekker, H.; Berendsen, H. J.; Fraaije, J. G. LINCS: a linear constraint solver for molecular simulations. *J. Comput. Chem.* **1997**, *18*, 1463−1472.

(36) Berendsen, H. J.; Postma, J. V.; Van Gunsteren, W. F.; DiNola, A. R. H. J.; Haak, J. R. Molecular dynamics with coupling to an external bath. *J. Chem. Phys.* **1984**, *81*, 3684−3690.

(37) Basconi, J. E.; Shirts, M. R. Effects of temperature control algorithms on transport properties and kinetics in molecular dynamics simulations. *J. Chem. Theory Comput.* **2013**, *9*, 2887−2899.

(38) Hess, B.; van der Vegt, N. F. Hydration thermodynamic properties of amino acid analogues: a systematic comparison of biomolecular force fields and water models. *J. Phys. Chem. B* **2006**, *110*, 17616−17626.

(39) Shirts, M. R.; Pitera, J. W.; Swope, W. C.; Pande, V. S. Extremely precise free energy calculations of amino acid side chain analogs: Comparison of common molecular mechanics force fields for proteins. *J. Chem. Phys.* **2003**, *119*, 5740−5761.

(40) Ohtaki, H.; Radnai, T. Structure and dynamics of hydrated ions. *Chem. Rev.* **1993**, *93*, 1157−1204.

(41) Astashkin, A. V.; Raitsimring, A. M.; Caravan, P. Pulsed ENDOR study of water coordination to Gd3+ complexes in

DOI: 10.1021/acs.jpcb.7b11384
J. Phys. Chem. B 2018, 122, 1334−1344

orientationally disordered systems. *J. Phys. Chem. A* **2004**, *108*, 1990−2001.
(42) Raitsimring, A. M.; Astashkin, A. V.; Baute, D.; Goldfarb, D.; Caravan, P. W-band 17O pulsed electron nuclear double resonance study of gadolinium complexes with water. *J. Phys. Chem. A* **2004**, *108*, 7318−7323.
(43) Pollet, R.; Marx, D. Ab initio simulation of a gadolinium-based magnetic resonance imaging contrast agent in aqueous solution. *J. Chem. Phys.* **2007**, *126*, 181102.
(44) Yazyev, O. V.; Helm, L. Gadolinium (III) ion in liquid water: Structure, dynamics, and magnetic interactions from first principles. *J. Chem. Phys.* **2007**, *127*, 084506.
(45) Bühl, M.; Sieffert, N.; Partouche, A.; Chaumont, A.; Wipff, G. Speciation of La (III) Chloride Complexes in Water and Acetonitrile: A Density Functional Study. *Inorg. Chem.* **2012**, *51*, 13396−13407.
(46) Tongraar, A.; Tangkawanwanit, P.; Rode, B. M. A combined QM/MM molecular dynamics simulations study of nitrate anion (NO3-) in aqueous solution. *J. Phys. Chem. A* **2006**, *110*, 12918−12926.
(47) Fratiello, A.; Kubo, V.; Lee, R. E.; Schuster, R. E. Direct proton magnetic resonance cation hydration study of uranyl perchlorate, nitrate, chloride, and bromide in water-acetone mixtures. *J. Phys. Chem.* **1970**, *74*, 3726−3730.
(48) Aaberg, M.; Ferri, D.; Glaser, J.; Grenthe, I. Structure of the hydrated dioxouranium (VI) ion in aqueous solution. An x-ray diffraction and proton NMR study. *Inorg. Chem.* **1983**, *22*, 3986−3989.
(49) Bushuev, Y. G.; Usacheva, T. R.; Sharnin, V. A. Molecular dynamics simulations of 18-crown-6 aqueous solutions. *J. Mol. Liq.* **2016**, *224*, 825−831.
(50) Ouerfelli, N.; Das, D.; Latrous, H.; Ammar, M.; Oliver, J. Transport behavior of the lanthanide 152Eu (III), 153Gd (III) and 170Tm (III) and transplutonium element 254Es (III), 244Cm (III), 241Am (III), 249Cf (III) and 249Bk (III) ions in aqueous solutions at 298 K. *J. Radioanal. Nucl. Chem.* **2014**, *300*, 51−55.
(51) Belle, J. Oxygen and uranium diffusion in uranium dioxide (a review). *J. Nucl. Mater.* **1969**, *30*, 3−15.
(52) Bannan, C. C.; Calabró, G.; Kyu, D. Y.; Mobley, D. L. Calculating partition coefficients of small molecules in octanol/water and cyclohexane/water. *J. Chem. Theory Comput.* **2016**, *12*, 4015−4024.
(53) Garrido, N. M.; Queimada, A. J.; Jorge, M.; Macedo, E. A.; Economou, I. G. 1-Octanol/water partition coefficients of n-alkanes from molecular simulations of absolute solvation free energies. *J. Chem. Theory Comput.* **2009**, *5*, 2436−2446.
(54) Kim, H. S. A Monte Carlo simulation study of solvent effect on Ba^{2+} to Sr^{2+} ion mutation. *Phys. Chem. Chem. Phys.* **2000**, *2*, 2919−2923.

DOI: 10.1021/acs.jpcb.7b11384
J. Phys. Chem. B 2018, 122, 1334−1344